



Published in final edited form as:

*Neuron*. 2008 March 13; 57(5): 705–718.

## Rapid Activity-Dependent Modifications in Synaptic Structure and Function Require Bidirectional Wnt Signaling

Bulent Ataman<sup>\*</sup>, James Ashley<sup>\*,†</sup>, Michael Gorczyca<sup>\*,†</sup>, Preethi Ramachandran<sup>\*</sup>, Wernher Fouquet<sup>#</sup>, Stephan J. Sigrist<sup>#</sup>, and Vivian Budnik

<sup>\*</sup>Department of Neurobiology, University of Massachusetts Medical School, Worcester, MA

<sup>#</sup>Institut für Klinische Neurobiologie und Rudolf-Virchow-Zentrum, Universität Würzburg, D-97078 Würzburg, Germany

### Summary

Activity-dependent modifications in synapse structure play a key role in synaptic development and plasticity, but the signaling mechanisms involved are poorly understood. We demonstrate that glutamatergic *Drosophila* neuromuscular junctions undergo rapid changes in synaptic structure and function in response to patterned stimulation. These changes, which depend on transcription and translation, include formation of motile presynaptic filopodia, elaboration of undifferentiated varicosities, and potentiation of spontaneous release frequency. Experiments indicate that a bidirectional Wnt/Wg signaling pathway underlies these changes. Evoked activity induces Wnt1/Wg release from synaptic boutons, which stimulates both a postsynaptic DFz2 nuclear import pathway, as well as a presynaptic pathway involving GSK-3 $\beta$ /Shaggy. Our findings suggest that bidirectional Wg signaling operates downstream of synaptic activity to induce modifications in synaptic structure and function. We propose that activation of the postsynaptic Wg pathway is required for the assembly of the postsynaptic apparatus, while activation of the presynaptic Wg pathway regulates cytoskeletal dynamics.

### INTRODUCTION

Synaptic plasticity has been placed at the foundation of complex brain functions, such as learning and memory and the refinement of synaptic connections. In these processes, correlated changes in electrical activity lead to long-term modifications in synaptic efficacy, which are often accompanied by structural changes in synapse shape and/or number (Chklovskii et al., 2004; Kandel, 2001). Although understanding the mechanisms for the induction of these changes has been the focus of intense efforts, many of the mechanisms downstream of activity remain unclear.

An important breakthrough has been the realization that many of the secreted molecules that play fundamental roles in pattern formation during early development function later in the nervous system to signal synapse development and plasticity. These include brain-derived neurotrophic factor (BDNF), Bone Morphogenetic Protein (BMP) and Wnts (Lu, 2003; Marques, 2005; Speese and Budnik, 2007). However, the extent of their participation and

---

Corresponding Author: Vivian Budnik, Department of Neurobiology, University of Massachusetts Medical School, LRB, 364 Plantation St., Worcester, MA 01605-2324, Tel.: (508) 856-4415, Email: Vivian.budnik@umassmed.edu, FAX: (508)856-6636.

<sup>†</sup>these authors contributed equally to the work.

**Publisher's Disclaimer:** This is a PDF file of an unedited manuscript that has been accepted for publication. As a service to our customers we are providing this early version of the manuscript. The manuscript will undergo copyediting, typesetting, and review of the resulting proof before it is published in its final citable form. Please note that during the production process errors may be discovered which could affect the content, and all legal disclaimers that apply to the journal pertain.

the cellular processes they initiate are for the most part unclear. Recent studies demonstrate that members of the Wingless (also known as Wg)/Int (Wnt) family of secreted signaling proteins are pivotal players during differentiation of synapses (Ciani and Salinas, 2005; Speese and Budnik, 2007), and misregulation of Wnt signaling is associated with a number of cognitive disorders such as schizophrenia and Alzheimer's (De Ferrari and Moon, 2006). However, a potential involvement of Wnts in activity-dependent changes at synapses is just beginning to be recognized (Chen et al., 2006; Wayman et al., 2006). A microarray analysis of dentate gyrus genes regulated by induction of long-term potentiation (LTP) led to the identification of several members of Wnt transduction pathways. Further, interfering with Wnt function reduced the magnitude of late LTP (Chen et al., 2006).

Both activity and the Wg pathway influence the development of synapses at the *Drosophila* larval neuromuscular junction (NMJ) (Budnik et al., 1990; Mosca et al., 2005; Packard et al., 2002; Schuster et al., 1996b). The larval NMJ is continuously forming and stabilizing new synapses in order to maintain synaptic efficacy as the postsynaptic muscle cells grow in size (Griffith and Budnik, 2006). NMJ expansion is stimulated by chronic intensification of both motorneuron activity and Wnt-1 (Wg) signaling (Budnik et al., 1990; Mosca et al., 2005; Packard et al., 2002). Mutations that decrease *wg* or the gene encoding its receptor, D-Frizzled-2 (DFz2), result in underdeveloped NMJs containing fewer synaptic boutons. A subset of these boutons remain undifferentiated, lacking active zones and postsynaptic specializations (Packard et al., 2002).

Current observations suggest that Wg might operate in a bidirectional manner, as DFz2 receptors are present in both pre- and postsynaptic compartments (Packard et al., 2002). In postsynaptic muscles, Wg secretion by presynaptic boutons activates an unconventional pathway, the Frizzled Nuclear Import (FNI) Wg pathway, in which the DFz2 receptor is endocytosed, cleaved, and the C-terminal fragment (DFz2C) is translocated into the nucleus (Ataman et al., 2006; Mathew et al., 2005). The signal transduction pathway activated by Wg in the presynaptic compartment is less clear. Studies show that the Wnt/Wg family of proteins utilizes a divergent canonical pathway involving the regulation of the microtubule cytoskeleton through the action of glycogen synthase kinase 3 $\beta$  (GSK-3 $\beta$ /Shaggy (Sgg)) on microtubule-associated proteins (Ciani et al., 2004; Speese and Budnik, 2007). GSK-3 $\beta$  is enriched at presynaptic boutons, and mutations in *sgg* have a positive effect on bouton proliferation, consistent with Wg inhibition of GSK-3 $\beta$  activity. Moreover, mutations in *wg* and *sgg* result in opposing defects in presynaptic microtubule cytoskeleton organization (Franco et al., 2004; Packard et al., 2002).

Here we establish that activity-dependent modifications in synapse structure at the larval NMJ are not simply the result of chronic changes in activity levels throughout development. Rather, rapid changes leading to the formation of new synaptic structures can be elicited by acute stimulation. These rapid structural changes depend on bidirectional Wg signaling and new protein synthesis. Our results support the notion that Wg is released from synaptic boutons in an activity-dependent manner, and that Wg functions downstream of activity to regulate synapse development and function. Thus, these studies establish a mechanistic link between acute activity changes and modifications in synaptic structure, and identify an important transduction cascade underlying these changes.

## RESULTS

### Activity induces rapid changes in synaptic structure

As in mammalian synapses, developmental changes in presynaptic activity have a substantial influence on the expansion of the *Drosophila* NMJ. Alterations that increase excitability throughout development result in enhanced proliferation of synaptic boutons, and this

phenotype can be rescued by mutations that lower excitability (Budnik et al., 1990; Mosca et al., 2005). The mechanisms by which enhanced presynaptic activity induce these morphological changes are still poorly understood. Moreover, it is unclear whether these changes arise as a result of long-term exposure to augmented activity during development, or whether acute activity is sufficient to regulate synaptic structure.

To address the latter question directly preparations expressing a membrane tethered GFP (mCD8-GFP) in motoneurons were imaged live before and after acute intervals of stimulation induced by high  $K^+$  depolarization paradigms. Spaced depolarization, in a pattern similar to that required to induce morphological changes in dendritic spines in mammalian hippocampal cultures (Wu et al., 2001), was found to be most effective in inducing rapid changes. Two striking changes were observed after repetitive, spaced depolarizations, consisting of 4–5 high (90 mM)  $K^+$ -pulses spaced by 15 min of rest (Fig. 1B). First, after approximately 2 hr from the beginning of the stimulation paradigm numerous, short, filopodia-like structures began to extend and retract from the NMJ with a time course of minutes (Fig. 1A, D and supplementary movie). These filopodia were 0.5 to 5.5  $\mu\text{m}$  long (average  $2.44 \pm 0.15 \mu\text{m}$ ;  $n=47$ ), and remained at their maximal length from 4 sec to over 100 sec (average =  $33.8 \pm 3.9$  sec;  $n=33$ ).

Many of these filopodia-like processes, which we termed synaptopods, appeared from the stretch of neurite between two boutons, but some also appeared to emerge from boutons themselves. Synaptopods could also be observed in unstimulated controls, or immediately after dissection, although their frequency was significantly lower (Fig. 1C), and they were much shorter ( $1.12 \pm 0.13 \mu\text{m}$ ;  $n=23$ ) compared to those observed after stimulation ( $2.44 \pm 0.15 \mu\text{m}$ ;  $n=47$ ). Synaptopods were usually not preserved by fixation, limiting their study to live preparations.

We also observed the appearance of synaptic varicosities that were often large and quite rounded (Fig. 2A top row; arrows). Unlike synaptopods, we were able to preserve these varicosities by our fixation protocol (Fig. 2A bottom row). However, similar to synaptopods the thin process connecting them to the main arbor was most often destroyed by fixation. Our ability to fix the newly formed varicosities allowed us to determine their nature by using a number of synaptic markers. Notably, they were devoid of postsynaptic proteins, such as Discs-Large (DLG; Fig. 2A bottom right panel, B, C arrows) or glutamate receptors (GluRs; Fig. 2F left panel arrows), and they rarely contained active zone markers such as nc82/Brp (Kittel et al., 2006b) (Fig. 2F right panel). In contrast, they were labeled with synaptic vesicle markers such as Cysteine String Protein (CSP) (Zinsmaier et al., 1994) (Fig. 2D arrows) and Synapsin (not shown). These varicosities resembled a certain type of synaptic bouton previously referred to as a “ghost bouton” (Ataman et al., 2006), which contains synaptic vesicles, but lacks active zones and postsynaptic structures. Ghost boutons have been shown to increase substantially in number upon genetically interfering with the Wg pathway at the NMJ, and in that case their appearance is accompanied by a dramatic decrease in normal bouton number (Ataman et al., 2006; Packard et al., 2002). Here, upon spaced stimulation ghost boutons formed *de novo*, and did not arise from retraction of existing boutons (Fig. 2A, E; Suppl. Fig. 1A). Therefore, these ghost boutons likely represent an undifferentiated bouton state, as they lack both pre- and postsynaptic specializations. Indeed, ghost boutons are also observed in unstimulated wild type preparations, albeit at very low frequency (Ataman et al., 2006). Thus, acute depolarization induces rapid changes in synaptic structure.

To determine if the formation of synaptopods represented a normal physiological process during NMJ growth, and whether ghost boutons developed into mature boutons, we imaged wild type unstimulated NMJs through the cuticle of intact early third instar larvae. NMJs were labeled by expressing mCD8-GFP or myristylated-mRFP (myr-mRFP) in motoneurons. In some experiments larvae also expressed either a postsynaptic GFP-tagged GluRIIA transgene

driven by the endogenous promoter (Rasse et al., 2005), or a presynaptic GFP-tagged Brp transgene (Wagh et al., 2006). We observed several instances of motile synaptopods at these NMJs (Suppl. Movie 2), suggesting that they are a normal occurrence during NMJ development. In addition we observed the appearance of ghost boutons, which as expected, were labeled by presynaptic myr-mRFP but were virtually devoid of postsynaptic GluR clusters (Fig. 3A,C arrows) and Brp-positive active zones (Fig. 3 D, E arrows). To establish if ghost boutons eventually acquired GluR or Brp clusters, larvae were returned to the food, and the same NMJ imaged at 12–18 hr intervals until the beginning of pupariation. We found several instances in which ghost boutons acquired GluR (Fig. 3A, C arrows) or Brp (Fig. 3D, E) clusters *de novo*, and that the number of GluR clusters increased over time (Fig. 3B). Therefore, ghost boutons are likely to represent an immature synaptic bouton state, which can differentiate into a mature bouton over prolonged periods.

We also determined some of the cellular and physiological requirements for enhanced ghost bouton formation. Dissected samples were stimulated with different depolarization paradigms and/or in the presence of specific pharmacological agents. A frequent appearance of synaptopods and ghost boutons required at least 4–5 cycles of spaced depolarization (Fig. 2E red arrows; Fig. 4A). Fewer cycles of spaced stimulation or pseudo-massed stimulation (same total stimulation period consisting of longer high  $K^+$  depolarization times and fewer stimulation/rest cycles, (Fig. 1B; Fig. 4A) or eliminating  $Ca^{++}$  from the external solution (Fig. 4B) did not lead to an increase in ghost bouton formation.

The spaced stimulation dependency was reminiscent of the patterned training required for long-term plasticity in a variety of systems (Kogan et al., 1997; Maelshagen et al., 1998; Wu et al., 2001; Yu et al., 2006), a process that depends on transcription and new protein synthesis. As both of these phenomena require spaced stimulation, we examined whether activity-dependent ghost bouton formation also required transcription and translation. Bath application of either the transcriptional inhibitor actinomycin (5mM) or the translational inhibitor cycloheximide (100mM) during stimulation prevented the formation of ghost boutons (Fig. 4B). Thus, activity dependent synapse remodeling depends on transcription and translation.

Just blocking action potentials in neurons by shifting the temperature sensitive neuronal  $Na^+$  channel mutant *paralytic (para<sup>ts</sup>)* (Wu and Ganetzky, 1980) to restrictive temperature during high  $K^+$  stimulation prevented the formation of ghost boutons (Fig. 4C), even though high  $K^+$  depolarization should allow neurotransmitter release in the absence of action potentials. This observation indicates that neurotransmitter release is not the only factor mediating rapid activity-dependent synapse modification, but that normal action potentials are also required.

### Spaced stimulation potentiates spontaneous release frequency

We next determined the physiological consequences of spaced 5X  $K^+$  depolarization by recording from the postsynaptic muscles after the spaced depolarization paradigm. In these animals the frequency of spontaneous excitatory potentials (mEJPs) was increased on average by about 3-fold compared to controls (Fig. 5A, B), suggesting a presynaptic modification. Presynaptic potentiation was evaluated through a frequency potentiation index, which is arrived at by dividing the mEJP frequency after stimulation by the control mEJP frequency (Fig. 5C).

A small but significant increase in mEJP amplitude was also observed upon spaced depolarization (Fig. 5D). This might result from multiquantal release, changes in postsynaptic receptor function, or activity-dependent changes in the size of synaptic vesicles (Steinert et al., 2006). No change in the amplitude of nerve-evoked responses was observed (Suppl. Fig. 1B). This was not due to a change in quantal content, as determination of quantal content by failure analysis (Del Castillo and Katz, 1954; Petersen et al., 1997) revealed no differences between

5X K<sup>+</sup> stimulated and non-stimulated samples (quantal content in unstimulated samples was 1.3±0.12 vs. 1.3±0.07 in 5X K<sup>+</sup> stimulated samples; n=4 and 5 respectively).

To assess if the changes in NMJ morphology and physiology could be elicited by patterned stimulation of motor nerves at frequencies comparable to those observed upon endogenous activity (Budnik et al., 1990), we also stimulated motor nerves with patterned 10 Hz frequency and examined the consequences for mEJPs and NMJ structural changes. A precise spaced pattern of high frequency stimulation (5 stimulation cycles, each consisting of 5 min of stimulation (2 sec at 10 Hz interspersed by 3 sec rest) and 15 min of rest; Fig. 5F blue and black) was required to elicit mEJP frequency potentiation (Fig. 5B, C), and structural synapse dynamics, as illustrated by the rapid motility of synaptopods (Fig. 5E arrows). The average magnitude of these changes was only slightly smaller than the 5X K<sup>+</sup>-induced depolarization results in wild type (Fig. 5C). However, examining individual experiments in a probability plot indicated that the high frequency nerve stimulation paradigm was not as effective as the spaced K<sup>+</sup>-induced depolarization paradigm (Fig. 5B).

As an additional independent way to establish that the observations with K<sup>+</sup> depolarization were physiologically relevant in the intact organism, experiments were also carried out by stimulating undissected larvae. For these experiments larvae expressing the light activated channel Channelrhodopsin-2 (ChR2;(Nagel et al., 2002; Schroll et al., 2006)) were fed all-trans-retinal containing food and subjected to light stimulation paradigms using 470nm illumination from an LED controlled by a stimulator. Patterned light stimulation similar to the electrical stimulation paradigm (5 stimulation cycles, each consisting of 5 min of light stimulation [2 sec illumination interspersed by 3 sec rest] and 15 min of rest; Fig. 5F purple and black) indeed potentiated mEJP frequency on average to the same level as nerve stimulation (Fig. 5B, C), and induced structural synaptic changes including the formation of ghost boutons (Fig. 4A, 5G). Recording from the postsynaptic muscles of ChR2 expressing larvae, while subjecting them to the light paradigm, demonstrated that the light stimulation elicited bursts of synaptic activity which did not exceed 50 Hz, as previously reported (Fig. 5F; (Schroll et al., 2006)). It is also noteworthy that light-induced mEJP potentiation lasted for at least 2–3 hrs. Thus, an acute increase in activity by direct nerve stimulation in dissected preparations or by light in ChR2- expressing intact larvae also leads to rapid modifications in synaptic structure and function. These observations also provide compelling evidence that the changes induced by high K<sup>+</sup> depolarization are physiologically relevant.

### Rapid activity-dependent changes in synaptic structure and function depend on Wg signaling

The similarity between ghost boutons observed upon spaced stimulation and those found in mutations that interfere with the Wg pathway led us to investigate a potential relationship between the activity-dependent changes described above and Wg signaling. Reducing Wg dosage by using heterozygous *wg<sup>ts/+</sup>* mutants shifted to restrictive temperature for 16 hr prior to dissection, or homozygous *wg<sup>l</sup>* hypomorphic mutants, completely prevented the observed increase in ghost bouton formation (Fig. 6A blue; compare to red) upon spaced 5X K<sup>+</sup> depolarization. This phenotype could be rescued by expressing Wg in motorneurons in the *wg<sup>ts/+</sup>* mutant background (Fig. 6A green). These changes were not simply due to a decreased excitability in *wg<sup>ts/+</sup>* mutants, since 0X K<sup>+</sup> *wg<sup>ts/+</sup>* larvae had mEJP frequency and amplitude as well as EJP amplitudes which were undistinguishable from wild type controls (Fig. 6D and Suppl. Fig. 1C).

Enhancing Wg secretion by overexpressing a *wg* transgene in motorneurons (*c380/+;UAS-Wg/+*) resulted in an increase in ghost boutons upon 5X K<sup>+</sup> spaced depolarization similar to wild type (Fig. 6A orange; compare to red). However, in NMJs overexpressing Wg in motorneurons, only 3 cycles of spaced stimulation (compared to the usual 5 in wild type) were

sufficient to enhance ghost bouton formation, quite unlike wild type NMJs with 3 cycles (Fig. 6A orange; compare to red). This enhancement was again suppressed by reducing *wg* dosage in *c380/+; wg<sup>ts</sup>/+*; *UAS-Wg/+* larvae (Fig. 6A green). The effect of overexpressing *Wg* in motorneurons was unlikely to result from increased excitability at these NMJs, as mEJP amplitude was not significantly different in 0X K<sup>+</sup> wild type and *UAS-Wg-pre* controls (Fig. 6D). Further, these larvae actually had a small but statistically significant decrease in EJP amplitude (Suppl. Fig. 1C). Thus, spaced depolarization induces ghost bouton formation in a *Wg*-dependent fashion, and enhancing *Wg* secretion can bypass some of the stimulation requirements for inducing ghost bouton formation.

We next examined whether the potentiation in mEJP frequency observed upon spaced 5X K<sup>+</sup> stimulation was also dependent on *Wg* signaling. Notably, this potentiation was prevented by reducing *wg* gene dosage (Fig. 6 B, C blue). When stimulated NMJs overexpressing *Wg* in motorneurons were compared to stimulated wild type NMJs, on average there was no statistically significant difference in the mEJP frequency (Fig. 6C orange). However, many stimulated NMJs overexpressing *Wg* in motorneurons displayed a significant shift towards higher mEJP frequencies when comparing individual experiments in a probability plot (Fig. 6B), further indicating that *Wg* release is involved in this potentiation. Interestingly, mEJP amplitude was also increased in all genotypes, suggesting that unlike mEJP frequency, the increase in mEJP amplitude did not depend on *Wg* (Fig. 6D). Just as wild type stimulation, there was also no significant change in evoked EJP amplitude (Suppl. Fig 1C). Thus the induction of ghost boutons and mEJP frequency potentiation after spaced 5X K<sup>+</sup> depolarization depends on the *Wg* pathway.

### Acute depolarization enhances *Wg* secretion

The suppression of activity-dependent structural and functional modifications by reducing *wg* dosage and the partial bypass of the stimulation requirements by increasing presynaptic *Wg* levels suggested that presynaptic activity might regulate *Wg* secretion. A measure of *Wg* release can be obtained by calculating the mean intensity of *Wg* staining within the immediate postsynaptic volume (as defined by the extent of DLG immunoreactivity and exclusion of the labeling by the presynaptic membrane marker anti-HRP (Jan and Jan, 1982) (Fig. 7A) by using 3D volumetric quantification of confocal stacks. Consistent with our hypothesis, the mean intensity of *Wg* immunoreactivity in the postsynaptic junctional volume displayed a small but statistically significant increase upon spaced 5X K<sup>+</sup> depolarization (Fig. 7A, B; Suppl. Fig. 2). This effect was suppressed by eliminating Ca<sup>++</sup> from the external solution (Fig. 7B). The levels of secreted postsynaptic *Wg* upon 5X K<sup>+</sup> depolarization was also substantially reduced when neurotransmitter release was temporally blocked (Fig. 7C, blue). This was achieved by expressing a temperature sensitive dominant-negative Dynamin transgene (*Shibire-DN<sup>ts</sup>*; *ShiDN<sup>ts</sup>*) (Kitamoto, 2001) in motorneurons and shifting the samples from permissive temperature to restrictive temperature, which blocks neurotransmission in a reversible manner by interfering with vesicle recycling (Koenig and Ikeda, 1989) (Fig. 7C, blue; controls in Suppl. Fig. 3C). Similarly, the secretion of *Wg* was also substantially reduced by blocking action potentials in *para<sup>ts1</sup>* mutants shifted to restrictive temperature (Fig. 7C, blue). Notably, the levels of presynaptic *Wg* did not change significantly after 5X K<sup>+</sup> depolarization (Fig. 7B, red) suggesting that, as demonstrated by studies of peptidergic vesicles (Shakiryanova et al., 2006) activity might induce the mobilization of vesicles into active terminals. This notion is also consistent with the observation that in *ShiDN<sup>ts</sup>* and *para<sup>ts1</sup>* synapses, there was a decrease in presynaptic *Wg* (Fig. 7C, red). Thus, activity regulates rapid synapse remodeling, most likely by stimulating *Wg* release from presynaptic boutons in a Ca<sup>++</sup>-dependent manner.

## Acute and chronic alterations in electrical activity modulate the postsynaptic Wnt Frizzled Nuclear Import pathway at the NMJ

The above observations demonstrated that NMJs can undergo rapid structural changes in response to activity in a Wg-dependent fashion. A short-term consequence of these changes is the formation of ghost boutons, which lack postsynaptic proteins and structures. Earlier studies have demonstrated that in postsynaptic muscles Wg secretion activates the postsynaptic FNI pathway (Mathew et al., 2005). Mutations that interfere with this pathway reduce DFz2C import into postsynaptic muscle nuclei. In contrast, enhancing Wg secretion from motorneurons leads to substantial increase in nuclear DFz2C entry. Therefore, if increased activity enhances Wg secretion we would expect to observe that acute spaced stimulation should result in augmentation of nuclear DFz2C entry. We found that the number of intranuclear DFz2C spots was significantly higher upon 5X K<sup>+</sup> spaced depolarization (Fig. 8A).

We also tested the effects of blocking activity on DFz2C nuclear import by expressing ShiDN<sup>ts</sup> in motorneurons and shifting the larvae to restrictive temperature for various time periods. Blocking neurotransmitter release significantly reduced the number of DFz2C nuclear spots (Fig. 8B). This decrease in nuclear DFz2C import was a function of the duration of the neurotransmitter block. While blocking synaptic transmission for 90 min before dissection led to a small but significant reduction in nuclear DFz2C import, increasing cumulative durations of the temperature shift led to increasingly larger reductions in nuclear DFz2C import when compared to their wild type controls (Fig. 8B; temperature controls in Suppl. Fig. 3A). A similar reduction in DFz2C nuclear import was observed when action potentials in neurons were blocked by shifting *para<sup>ts</sup>* mutants to restrictive temperature (Fig. 8C). In these mutants K<sup>+</sup> depolarization would still elicit neurotransmitter release, suggesting that neurotransmitter release is not the only relevant process in the regulation of muscle DFz2C nuclear import. Thus levels of activity are directly correlated to the magnitude of DFz2C nuclear import.

A prediction of the above experiments is that chronic changes in activity should also lead to an increase in DFz2C nuclear import. This was tested by examining the hyperexcitable mutant *eag Sh* which was previously reported to stimulate the development of new synaptic boutons and active zones (Budnik et al., 1990; Jia et al., 1993). We found a dramatic increase in the number of nuclear DFz2C spots in *eag Sh* mutants (Fig. 8D, E). This enhancement was completely suppressed by reducing *wg* gene dosage in a heterozygous *wg* mutant, corroborating a dependency on FNI (Fig. 8D). An enhancement in DFz2C nuclear import was also found when larvae expressing ChR2 in motorneurons were stimulated by the light paradigm every 12 hr for the last 3 days of larval development (Fig. 8D). Thus, the acute changes in DFz2C nuclear import are further enhanced by augmenting activity in a chronic fashion.

## Rapid changes in presynaptic structure and function depend on GSK-3 $\beta$ /Sgg function in motorneurons

While the above results implicate a role for the postsynaptic Wg signaling pathway, most of the immediate changes we observed in synaptic structure were presynaptic. Presynaptic activation of a Wg pathway has been previously suggested through studies of the Shaggy/GSK-3 $\beta$  kinase (Franco et al., 2004; Packard et al., 2002). A major outcome of activation of the canonical and divergent canonical Wnt/Wg pathways is the inhibition of GSK-3 $\beta$ . The latter pathway has been implicated in cytoskeletal rearrangements during axonal remodeling and in the differentiation of presynaptic terminals (Ciani and Salinas, 2005; Speese and Budnik, 2007). This regulation is thought to occur through GSK-3 $\beta$ -dependent phosphorylation of microtubule associated proteins (MAPs), which in turn influence microtubule dynamics (Goold and Gordon-Weeks, 2004). Studies have also provided evidence that GSK-3 $\beta$  is localized to

actin-rich regions of the growth cone where it controls axonal growth (Eickholt et al., 2002). Studies at the larval NMJ demonstrate that GSK-3 $\beta$  is enriched within presynaptic terminals, and that mutations in the GSK-3 $\beta$  gene *sgg* result in alterations in bouton number and the organization of the microtubule cytoskeleton (Franco et al., 2004; Packard et al., 2002). These changes are, as expected from the inhibition of GSK-3 $\beta$  by Wg signaling, the opposite of those elicited by mutations in Wg.

The Wg-dependent modifications in the structure of presynaptic arbors upon spaced stimulations raised the question of whether Sgg, a key component of Wg signaling, was involved in this process. This question was investigated by enhancing or decreasing Sgg function specifically in motoneurons, either by presynaptic expression of a full-length Sgg transgene, which was previously shown to antagonize Wg signaling (Bourouis 2002), or by presynaptic expression of a dominant-negative kinase-null Sgg transgene (SggDN) which was reported to phenocopy *sgg* loss-of-function at the NMJ (Franco et al., 2004). Presynaptic expression of Sgg completely suppressed the activity-dependent induction of ghost boutons (Fig. 8F blue; compare to red). In contrast, inhibiting presynaptic Sgg by expressing the SggDN transgene did not interfere with ghost bouton formation upon 5X K<sup>+</sup> spaced depolarization, although this increase was slightly less robust than wild type (Fig. 8F orange). Notably, in agreement with the notion that inhibiting Sgg mimics the activation of the Wg pathway, the number of ghost boutons was significantly increased even upon just 3 cycles of stimulation upon expressing SggDN in motoneurons as compared to the requirement of 4–5 cycles of stimulation in wild type (Fig. 8F orange). Thus, while activity activates the FNI pathway in postsynaptic muscles, our results are consistent with a concomitant activation of a divergent canonical Wg pathway mediated by Sgg in the presynaptic motoneuron.

We also determined if potentiation of mEJP frequency was influenced by enhancing or decreasing Sgg activity. Overexpressing Sgg resulted in an increase in mEJP frequency after 5X K<sup>+</sup> spaced stimulation, although this increase was less than 2-fold compared with a 3-fold enhancement in stimulated wild type larvae (Fig. 8G, I blue; compare to red). Interestingly, potentiation of mEJP frequency was augmented by almost 4-fold upon presynaptic expression of SggDN (Fig. 8G, I orange). These results are in agreement with the previously suggested hypothesis that Wg activates a canonical or divergent canonical presynaptic pathway that leads to Sgg inhibition. Increasing Sgg function partially or completely bypassed Wg-dependent inhibition, preventing the activity-dependent increase in ghost boutons, and decreasing mEJP potentiation. Reducing Sgg function in presynaptic motoneurons did not interfere with activity-dependent potentiation of mEJP frequency and enhanced ghost bouton formation close to wild type levels (Fig. 8F, G, I). Similar to all other genotypes (Fig. 6D), Sgg transgenic flies also exhibited a small but significant increase in mEJP amplitude upon spaced 5X K<sup>+</sup> depolarization (Fig. 8J). These observations provide evidence for simultaneous activation of pre- and postsynaptic Wg signaling in response to patterned activity and place a bidirectional Wg pathway as a critical downstream component of activity-dependent synapse remodeling.

## DISCUSSION

Understanding how neuronal circuits can be modified in the mature brain requires knowledge of the mechanisms by which synapses can be shifted from a relatively stable state to a dynamic condition that allows new synaptic growth or elimination. Here we have shown that rapid activity-dependent changes in synapse development and function can be induced at the *Drosophila* glutamatergic NMJs in a process that depends on spaced stimulation, akin to changes observed in dendritic spines of hippocampal neurons in culture (Yao et al., 2006). During the postembryonic period after initial formation of synaptic contacts, synaptic boutons continuously proliferate in conjunction with changes in postsynaptic target size (Griffith and Budnik, 2006). Chronic increases in activity, induced by mutations in ion channels,



significantly enhance the formation of new synaptic boutons (Budnik et al., 1990; Schuster et al., 1996a). Here we demonstrate that activity-dependent changes are not simply the result of a developmental elevation in overall neuronal excitability, but rather that the ability of synapses to respond to changes in activity through structural and functional dynamics is an acute process, which is rapidly established upon patterned stimulation. Further, we have identified an important downstream mechanism, the Wnt pathway, which links activity-dependent changes to structural and functional synaptic modifications.

Together, the findings that (1) activity can induce Wg release from presynaptic boutons, (2) patterned activity elicits acute changes in synapse function and structural dynamics in a Wg-dependent fashion, (3) increasing Wg secretion can bypass some of the activity requirements, (4) intensifying or blocking activity has a corresponding influence on DFz2C entry into the nucleus in the postsynaptic muscle cell, and (5) activity modifications can be completely or partially suppressed by modulating GSK-3 $\beta$  in the presynaptic cell, demonstrate that bidirectional Wg signaling is a key downstream mediator of activity-dependent synaptic plasticity.

We propose the following model on bidirectional regulation of synapse structure and function by the Wg pathway (Fig. 8H). Spaced stimulation results in the release of Wg by presynaptic boutons, which binds to DFz2 receptors present both pre- and postsynaptically (Packard et al., 2002). In the presynaptic compartment, Wg release likely regulates cytoskeletal dynamics through inhibition of Sgg activity, leading to synaptopod dynamics and formation of ghost boutons in a process that depends on transcriptional and/or translational activation. In the postsynaptic compartment Wg release activates the FNI pathway, resulting in DFz2C cleavage and import into the nucleus where it may induce the transcription of synaptic genes (Fig. 8H). Disrupting the Wg pathway during synapse development dampens the maturation of new synaptic boutons resulting in NMJs containing fewer mature boutons as well as a larger number of undifferentiated ghost boutons (Ataman et al., 2006; Packard et al., 2002). While our results are consistent with this model, alternative possibilities must be also considered. For example, changes in Wg signaling might alter excitability (beyond the parameters examined in this study) and these changes might trigger parallel transduction pathways that modulate synaptic structure and function. In addition, it is unlikely that Wg alone is responsible for all activity-dependent mechanisms. For example, the participation of a retrograde BMP signaling pathway in the regulation of synaptic bouton proliferation is well-established (Marques, 2005). It is highly likely that multiple signaling pathways, including Wg, BMPs and others collaborate in the orchestration of activity-dependent synapse modifications.

### Acute changes in synapse structure and function

The most striking structural changes we observed were the *de novo* formation of synaptopods and ghost boutons. Although the nature of synaptopods is unclear, they might represent an initial stage during synaptic bouton formation like the filopodia observed at dendritic spines in normal animals and in response to activity (Niell et al., 2004; Yuste and Bonhoeffer, 2004). However, in our studies we never observed a transition from synaptopod to bouton. Another possibility is that they might correspond to exploratory structures that convey a signal to pre- and/or postsynaptic sites. This function has also been suggested for dendritic filopodia (Dunaevsky and Mason, 2003; Yuste and Bonhoeffer, 2004) as well as for growth cone filopodia prior to target innervation (Kalil and Dent, 2005).

Ghost boutons, on the other hand, represent rapid *de novo* formation of undifferentiated boutons. Their formation is not the result of retraction of mature boutons. They are found to contain synaptic vesicles, but virtually lack pre- and postsynaptic specializations. Our live imaging studies showed that these boutons could acquire postsynaptic GluR and presynaptic Brp clusters over a relatively long period after their initial formation.

The above morphological changes required transcription and/or translation, akin to late LTP and long-term memory (Kandel, 2001), but the step(s) at which they are required remains unclear. Potential scenarios include an activity-dependent increase in *wg* mRNA or Wg protein synthesis as observed in the mammalian brain (Wayman et al., 2006). They could also involve the activation of alternative pathways such as PKA and CREB-dependent mechanisms (Davis et al., 1998; Davis et al., 1996; Wayman et al., 2006).

Previous live imaging studies of wild type intact larval NMJs did not report the occurrence of synaptopods and ghost boutons (Zito et al., 1999). However, in that study a postsynaptic marker (mCD8-GFP-Sh) was used to label the NMJ, and thus synaptopods and ghost boutons would not have been observed.

We also observed a Wg-dependent potentiation of mEJP frequency after spaced stimulation. An increased mEJP frequency has also been observed at the embryonic NMJ upon high frequency stimulation, although the accompanying structural changes were not examined in that preparation (Yoshihara et al., 2005). The potentiation of mEJP frequency that we observed did not result from the addition of ghost boutons, as ghost boutons only rarely contain active zones (Ataman et al., 2006). In addition, it occurred without any change in the number of nc82/Brp puncta in existing boutons (data not shown), suggesting that this potentiation is unlikely to emerge from the recruitment of new active zones. However, nc82/Brp is thought to label just the T-bar component of the active zone (Kittel et al., 2006a), and many active zones lack T-bars (Atwood et al., 1993). Thus, this possibility cannot be completely ruled out. Alternatively, the increase in mini frequency might arise from unsilencing of existing synapses as shown in mammals (Yao et al., 2006) or from changes in their intrinsic properties.

Potentiation of spontaneous release frequency has been widely implicated in synapse maturation (Zucker, 2005). At the *Xenopus* NMJ repetitive neuron stimulation also results in the potentiation of spontaneous synaptic activity which is associated with synapse maturation (Lo et al., 1991). Expressing SynCaM, a homophilic cell adhesion molecule that drives synaptic maturation, also increases the frequency of spontaneous release (Biederer et al., 2002). At the *Drosophila* embryonic NMJ mutations that block the potentiation of spontaneous release frequency, such as mutants lacking both D $\text{GluRIIA}$  and D $\text{GluRIIB}$ , as well as mutations in *syntaxin*, and *synaptotagmin IV*, exhibit abnormal NMJ development. These mutants all show a lack of presynaptic maturation, as demonstrated by a maintained growth cone structure (Yoshihara et al., 2005). In the mammalian nervous system spontaneous release has been shown to regulate postsynaptic local protein synthesis which is thought to stabilize synaptic function (Chung and Kavalali, 2006). Thus, the mEJP frequency potentiation observed here may play an initial role in postsynaptic maturation.

Importantly, spaced stimulation also induced a small but significant increase in mEJP amplitude that did not depend on Wg. Thus, activity is likely to regulate additional Wg-independent pathways. For example, elevated  $\text{Ca}^{++}$  induces the mobilization of vesicles to release sites, thereby increasing the number of active zones containing more than one docked vesicle, and thus eliciting multi-quantal release (Koenig et al., 1993). Recent studies have also suggested an activity-dependent increase in the size of synaptic vesicles (Steinert et al., 2006). However, the change in mEJP amplitude was not accompanied by modifications in the amplitude of evoked responses, as expected if quantal size was larger, and further, we did not see a change in quantal content as determined by failure analysis.

### Activity-dependent Wg release and role of Wg in functional and structural synaptic changes

Wg secretion was also found to be regulated by activity. Spaced depolarization increased the levels of Wg at the postsynaptic area, and conversely, temporally blocking activity in *para<sup>ts1</sup>* and by expressing ShiDN<sup>ts</sup> in motorneurons decreased secreted Wg. Given that diminishing

*wg* gene dosage prevented the rapid activity-dependent changes, these results suggest that Wg operates downstream of activity to promote these changes. This conclusion is further supported by the observation that increasing Wg secretion by overexpressing Wg in motorneurons, or activating the presynaptic Wg pathway by expressing a SggDN in motorneurons, partially bypassed the requirement for activity.

Notably, we found that activity-dependent Wg release did not decrease presynaptic Wg levels. In contrast, reducing Wg release through *para<sup>ts1</sup>* and ShiDN<sup>ts</sup> diminished Wg levels in presynaptic boutons. This is in agreement with recent studies documenting activity-dependent trafficking of peptidergic vesicles at the *Drosophila* NMJ (Shakiryanova et al., 2005; Shakiryanova et al., 2006). In resting terminals peptidergic vesicles are relatively immobile, but activity induces a rapid mobilization of these vesicles to active terminals. Alternatively (or in addition), activity (or lack thereof) might influence the transcription and/or translation of Wg, consistent with the requirement of transcription and/or translation in ghost bouton formation.

### Wnts and activity at mammalian synapses

Tetanic stimulation in hippocampal slices induces NMDA receptor-dependent release of Wnt3a by postsynaptic cells, the translocation of  $\beta$ -Catenin into the nucleus, and the upregulation of Wnt target genes (Chen et al., 2006). Further, altering Wnt signaling levels caused corresponding changes in the magnitude of LTP (Ahmad-Annur et al., 2006; Chen et al., 2006). Members of the Wnt pathway are also involved in activity-dependent dendritic arborization (Wayman et al., 2006; Yu and Malenka, 2003). Activation of an NMDA receptor- and  $\text{Ca}^{++}$ -dependent pathway resulted in CREB responsive transcription of Wnt-2, through activation of CaM kinase kinase (CaMKK), that coupled neuronal activity with dendritic development (Wayman et al., 2006). Similarly, other studies suggest that the enhancement of dendritic growth induced by depolarization requires  $\beta$ -Catenin and an increased Wnt release (Yu and Malenka, 2003).

To date, mammalian Wnts have been shown to be secreted by postsynaptic cells (Ciani and Salinas, 2005). However, multiple members of the Wnt family exist both in *Drosophila* and in mammalian systems, and different members might be released by different synaptic compartments. Alternatively, the anterograde, retrograde, or autocrine nature of Wnt signaling at synapses might have changed through evolution.

Notably, spaced, but not massed stimulation of cultured hippocampal neurons and dentate gyrus explants resulted in the persistent extension of postsynaptic filopodia and spine-like structures in dendrites (Wu et al., 2001). As in our experiments, the induction of these structures depended on calcium and did not begin to appear until the 3<sup>rd</sup> – 4<sup>th</sup> spaced stimulation cycle (Wu et al., 2001). Spaced depolarization also led to an increase in mEPSC frequency thought to emerge from the activation of silent synapses (Yao et al., 2006). Our findings in this study indicate that the cellular processes underlying rapid activity-dependent changes in synaptic structure and function appear to be conserved in presynaptic arbors of the NMJ.

Our results also implicate presynaptic GSK-3 $\beta$  in the presynaptic compartment during rapid activity-dependent changes at the larval NMJ. GSK-3 $\beta$  is known to regulate microtubule and actin cytoskeletons. In the case of microtubules, it phosphorylates MAP1B and tau, thereby influencing microtubule stability (Goold and Gordon-Weeks, 2004). In agreement with those observations, GSK-3 $\beta$ /Sgg phosphorylates the *Drosophila* MAP1B-related protein Futsch (Gogel et al., 2006), and Futsch is required for Sgg function in synaptic growth (Franco et al., 2004). Further, in *sgg* mutants the number of bundled/stable microtubule loops within synaptic boutons were dramatically increased, exactly the opposite phenotype of *wg* mutants (Franco et al., 2004; Packard et al., 2002).

In summary, our studies demonstrate that rapid modifications in synapse structure and function can be elicited in glutamatergic synapses at the larval NMJ, and identify Wg signaling as a critical effector of activity-dependent synaptic plasticity. These studies also provide a prominent *in vivo* model system to examine structural and physiological consequences of acute activity in a genetically tractable organism.

## MATERIALS AND METHODS

### Fly strains

Flies were reared in standard *Drosophila* medium at 25°C, except where indicated. The following stocks were used (see Suppl. Material for strain details and number of samples for each experiment): Canton-S, *wg<sup>ts</sup>* (*wg<sup>IL114</sup>*), *wg<sup>1</sup>*, UAS-Wg, GluRIIA-GFP, UAS-Brp-GFP, *para<sup>ts1</sup>*, UAS-ShiDN<sup>ts</sup>, *eag<sup>1</sup> Sh<sup>133</sup>*, UAS-mCD8:GFP, UAS-Sgg, UAS-SggDN (A81T), UAS-ChR2 and the motorneuron Gal4 driver C380.

### Heat shock, high K<sup>+</sup> depolarization, and light stimulation paradigms

Precise stimulation paradigms are described in the Suppl. Materials. *wg<sup>ts</sup>/+* larvae reared at 17°C were shifted to 29°C for 16 hr prior to dissection. For UAS-ShiDN<sup>ts</sup> or *para<sup>ts1</sup>* the restrictive temperature (RET) was 32°C and the permissive temperature room temperature. High K<sup>+</sup> depolarization paradigms were performed using 90 mM K<sup>+</sup> HL3 (Roche et al., 2002) adjusted for osmolarity. 100 mM cycloheximide or 5 mM actinomycin (Sigma) were included in the normal and high K<sup>+</sup> HL3 in some experiments as indicated in the text. For the Channelrhodopsin-2 light paradigm, larvae were raised on 100 μM all-trans-retinal food and stimulated with multiple blue light (470nm) LEDs. Live imaging was conducted with a Zeiss Pascal or an Improvion spinning disc confocal microscope using a water immersion 25X (0.8 N.A.) objective.

### Immunocytochemistry

Primary antibodies were as follows (see Supplementary Material for details): anti-Wg, anti-DLG, anti-GluRIII, nc82, anti-CSP, anti-DFz2-C, and FITC- or Texas Red-conjugated anti-HRP. Imaging of fixed preparations was performed using a Zeiss Pascal confocal microscope. Quantification of secreted Wg was performed as in (Gorczyca et al., 2007) and described in the Suppl. Material.

### Quantification of nuclear DFz2C spots, ghost boutons and synaptopods

Measurements were done at muscles 6 and 7 abdominal segment 3. Intranuclear DFz2C spots and ghost boutons were quantified as in (Ataman et al., 2006; Mathew et al., 2005). Synaptopods were quantified from confocal images of live preparations. Statistical significance in two-way or multiple group comparisons was determined using a Student t-test and a one way ANOVA with a Tukey *post hoc* test respectively. Numbers in histograms represent mean. ±SEM.

### Live-imaging of intact larvae

Live imaging of undissected larvae was conducted in muscle 14, 30 and 27 as in (Rasse et al., 2005) and described in the Suppl. Material.

### Electrophysiology

Electrophysiological recordings were carried out as in (Ashley et al., 2005). For details on the stimulation paradigms see Suppl. Material.

## Supplementary Material

Refer to Web version on PubMed Central for supplementary material.

### ACKNOWLEDGEMENTS

We would like to thank Dr. Sean Speese for helpful comments on the manuscript, as well as the Budnik lab members, Dr. Marc Freeman and Dr. Scott Waddell for helpful discussions and advise. We also thank Mr. Francisco Urrea for help in the initial investigation of electrical stimulation paradigms. Supported by a grant from the National Institute of Mental Health MH070000 to VB. Core resources supported by the Diabetes Endocrinology Research Center grant DK32520 were also used. S.J.S. was supported by grants of the Deutsche Forschungsgemeinschaft (SI849/2-1, SFB581/B23).

### REFERENCES

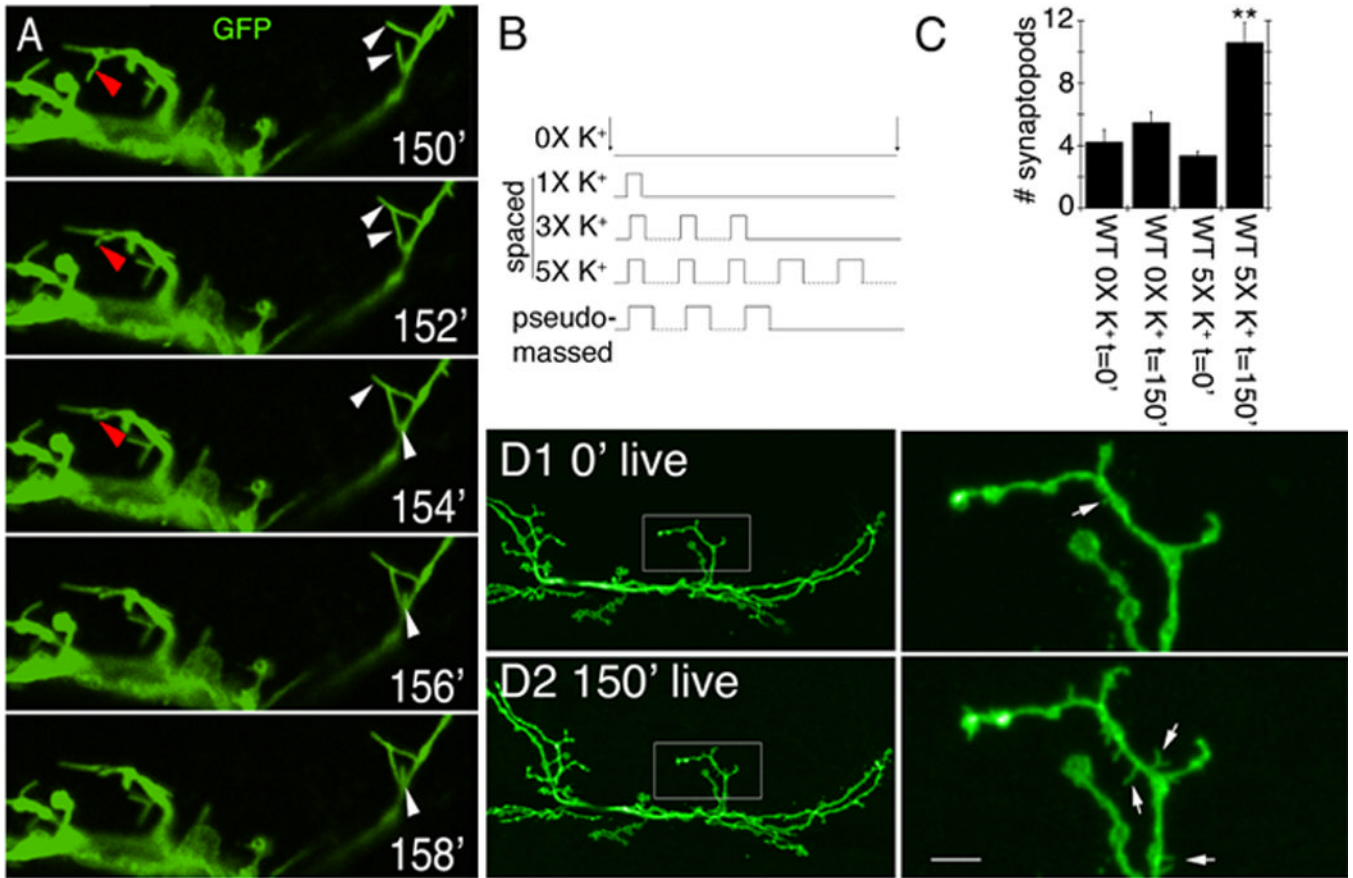
- Ahmad-Annuar A, Ciani L, Simeonidis I, Herreros J, Fredj NB, Rosso SB, Hall A, Brickley S, Salinas PC. Signaling across the synapse: a role for Wnt and Dishevelled in presynaptic assembly and neurotransmitter release. *J Cell Biol* 2006;174:127–139. [PubMed: 16818724]
- Ashley J, Packard M, Ataman B, Budnik V. Fasciclin II signals new synapse formation through amyloid precursor protein and the scaffolding protein dX11/Mint. *J Neurosci* 2005;25:5943–5955. [PubMed: 15976083]
- Ataman B, Ashley J, Gorczyca D, Gorczyca M, Mathew D, Wichmann C, Sigrist SJ, Budnik V. Nuclear trafficking of Drosophila Frizzled-2 during synapse development requires the PDZ protein dGRIP. *Proc Natl Acad Sci U S A* 2006;103:7841–7846. [PubMed: 16682643]
- Atwood HL, Govind CK, Wu CF. Differential ultrastructure of synaptic terminals on ventral longitudinal abdominal muscles in Drosophila larvae. *J Neurobiol* 1993;24:1008–1024. [PubMed: 8409966]
- Biederer T, Sara Y, Mozhayeva M, Atasoy D, Liu X, Kavalali ET, Sudhof TC. SynCAM, a synaptic adhesion molecule that drives synapse assembly. *Science* 2002;297:1525–1531. [PubMed: 12202822]
- Budnik V, Zhong Y, Wu CF. Morphological plasticity of motor axons in Drosophila mutants with altered excitability. *J Neurosci* 1990;10:3754–3768. [PubMed: 1700086]
- Chen J, Park CS, Tang SJ. Activity-dependent synaptic Wnt release regulates hippocampal long term potentiation. *J Biol Chem* 2006;281:11910–11916. [PubMed: 16501258]
- Chklovskii DB, Mel BW, Svoboda K. Cortical rewiring and information storage. *Nature* 2004;431:782–788. [PubMed: 15483599]
- Chung C, Kavalali ET. Seeking a function for spontaneous neurotransmission. *Nat Neurosci* 2006;9:989–990. [PubMed: 16871164]
- Ciani L, Krylova O, Smalley MJ, Dale TC, Salinas PC. A divergent canonical WNT-signaling pathway regulates microtubule dynamics: dishevelled signals locally to stabilize microtubules. *J Cell Biol* 2004;164:243–253. [PubMed: 14734535]
- Ciani L, Salinas PC. WNTs in the vertebrate nervous system: from patterning to neuronal connectivity. *Nat Rev Neurosci* 2005;6:351–362. [PubMed: 15832199]
- Davis GW, DiAntonio A, Petersen SA, Goodman CS. Postsynaptic PKA controls quantal size and reveals a retrograde signal that regulates presynaptic transmitter release in Drosophila. *Neuron* 1998;20:305–315. [PubMed: 9491991]
- Davis GW, Schuster CM, Goodman CS. Genetic dissection of structural and functional components of synaptic plasticity. III. CREB is necessary for presynaptic functional plasticity [see comments]. *Neuron* 1996;17:669–679. [PubMed: 8893024]
- De Ferrari GV, Moon RT. The ups and downs of Wnt signaling in prevalent neurological disorders. *Oncogene* 2006;25:7545–7553. [PubMed: 17143299]
- Del Castillo J, Katz B. Quantal components of the end-plate potential. *J Physiol* 1954;124:560–573. [PubMed: 13175199]
- Dunaevsky A, Mason CA. Spine motility: a means towards an end? *Trends Neurosci* 2003;26:155–160. [PubMed: 12591218]
- Eickholt BJ, Walsh FS, Doherty P. An inactive pool of GSK-3 at the leading edge of growth cones is implicated in Semaphorin 3A signaling. *J Cell Biol* 2002;157:211–217. [PubMed: 11956225]

- Franco B, Bogdanik L, Bobinnec Y, Debec A, Bockaert J, Parmentier ML, Grau Y. Shaggy, the homolog of glycogen synthase kinase 3, controls neuromuscular junction growth in *Drosophila*. *J Neurosci* 2004;24:6573–6577. [PubMed: 15269269]
- Gogel S, Wakefield S, Tear G, Klambt C, Gordon-Weeks PR. The *Drosophila* microtubule associated protein Futsch is phosphorylated by Shaggy/Zeste-white 3 at an homologous GSK3beta phosphorylation site in MAP1B. *Mol Cell Neurosci* 2006;33:188–199. [PubMed: 16949836]
- Goold RG, Gordon-Weeks PR. Glycogen synthase kinase 3beta and the regulation of axon growth. *Biochem Soc Trans* 2004;32:809–811. [PubMed: 15494021]
- Gorczyca D, Ashley J, Speese S, Gherbesi N, Thomas U, Gundelfinger E, Gramates LS, Budnik V. Postsynaptic membrane addition depends on the Discs-Large-interacting t-SNARE Gtaxin. *J Neurosci* 2007;27:1033–1044. [PubMed: 17267557]
- Griffith LC, Budnik V. Plasticity and second messengers during synapse development. *Int Rev Neurobiol* 2006;75:237–265. [PubMed: 17137931]
- Jan LY, Jan YN. Antibodies to horseradish peroxidase as specific neuronal markers in *Drosophila* and in grasshopper embryos. *Proc Natl Acad Sci U S A* 1982;79:2700–2704. [PubMed: 6806816]
- Jia XX, Gorczyca M, Budnik V. Ultrastructure of neuromuscular junctions in *Drosophila*: comparison of wild type and mutants with increased excitability. *J Neurobiol* 1993;24:1025–1044. [PubMed: 8409967][published erratum appears in *J Neurobiol* 1994 Jul;25(7):893-5]
- Kalil K, Dent EW. Touch and go: guidance cues signal to the growth cone cytoskeleton. *Curr Opin Neurobiol* 2005;15:521–526. [PubMed: 16143510]
- Kandel ER. The molecular biology of memory storage: a dialogue between genes and synapses. *Science* 2001;294:1030–1038. [PubMed: 11691980]
- Kitamoto T. Conditional modification of behavior in *Drosophila* by targeted expression of a temperature-sensitive shibire allele in defined neurons. *J Neurobiol* 2001;47:81–92. [PubMed: 11291099]
- Kittel RJ, Hallermann S, Thomsen S, Wichmann C, Sigrist SJ, Heckmann M. Active zone assembly and synaptic release. *Biochem Soc Trans* 2006a;34:939–941. [PubMed: 17052232]
- Kittel RJ, Wichmann C, Rasse TM, Fouquet W, Schmidt M, Schmid A, Wagh DA, Pawlu C, Kellner RR, Willig KI, et al. Bruchpilot promotes active zone assembly, Ca<sup>2+</sup> channel clustering, and vesicle release. *Science* 2006b;312:1051–1054. [PubMed: 16614170]
- Koenig JH, Ikeda K. Disappearance and reformation of synaptic vesicle membrane upon transmitter release observed under reversible blockage of membrane retrieval. *J Neurosci* 1989;9:3844–3860. [PubMed: 2573698]
- Kogan JH, Frankland PW, Blendy JA, Coblenz J, Marowitz Z, Schutz G, Silva AJ. Spaced training induces normal long-term memory in CREB mutant mice. *Curr Biol* 1997;7:1–11. [PubMed: 8999994]
- Lo YJ, Wang T, Poo MM. Repetitive impulse activity potentiates spontaneous acetylcholine secretion at developing neuromuscular synapses. *J Physiol (Paris)* 1991;85:71–78. [PubMed: 1757892]
- Lu B. BDNF and activity-dependent synaptic modulation. *Learn Mem* 2003;10:86–98. [PubMed: 12663747]
- Marques G. Morphogens and synaptogenesis in *Drosophila*. *J Neurobiol* 2005;64:417–434. [PubMed: 16041756]
- Mathew D, Ataman B, Chen J, Zhang Y, Cumberledge S, Budnik V. Wingless signaling at synapses is through cleavage and nuclear import of receptor DFrizzled2. *Science* 2005;310:1344–1347. [PubMed: 16311339]
- Mauelshagen J, Sherff CM, Carew TJ. Differential induction of long-term synaptic facilitation by spaced and massed applications of serotonin at sensory neuron synapses of *Aplysia californica*. *Learn Mem* 1998;5:246–256. [PubMed: 10454368]
- Mosca TJ, Carrillo RA, White BH, Keshishian H. Dissection of synaptic excitability phenotypes by using a dominant-negative Shaker K<sup>+</sup> channel subunit. *Proc Natl Acad Sci U S A* 2005;102:3477–3482. [PubMed: 15728380]
- Nagel G, Ollig D, Fuhrmann M, Kateriya S, Musti AM, Bamberg E, Hegemann P. Channelrhodopsin-1: a light-gated proton channel in green algae. *Science* 2002;296:2395–2398. [PubMed: 12089443]
- Niell CM, Meyer MP, Smith SJ. In vivo imaging of synapse formation on a growing dendritic arbor. *Nat Neurosci* 2004;7:254–260. [PubMed: 14758365]

- Packard M, Koo ES, Gorczyca M, Sharpe J, Cumberledge S, Budnik V. The *Drosophila* wnt, wingless, provides an essential signal for pre- and postsynaptic differentiation. *Cell* 2002;111:319–330. [PubMed: 12419243]
- Petersen SA, Fetter RD, Noordermeer JN, Goodman CS, DiAntonio A. Genetic analysis of glutamate receptors in *Drosophila* reveals a retrograde signal regulating presynaptic transmitter release. *Neuron* 1997;19:1237–1248. [PubMed: 9427247]
- Rasse TM, Fouquet W, Schmid A, Kittel RJ, Mertel S, Sigrist CB, Schmidt M, Guzman A, Merino C, Qin G, et al. Glutamate receptor dynamics organizing synapse formation in vivo. *Nat Neurosci* 2005;8:898–905. [PubMed: 16136672]
- Roche JP, Packard MC, Moeckel-Cole S, Budnik V. Regulation of synaptic plasticity and synaptic vesicle dynamics by the PDZ protein Scribble. *J Neurosci* 2002;22:6471–6479. [PubMed: 12151526]
- Schroll C, Riemensperger T, Bucher D, Ehmer J, Voller T, Erbguth K, Gerber B, Hendel T, Nagel G, Buchner E, Fiala A. Light-induced activation of distinct modulatory neurons triggers appetitive or aversive learning in *Drosophila* larvae. *Curr Biol* 2006;16:1741–1747. [PubMed: 16950113]
- Schuster CM, Davis GW, Fetter RD, Goodman CS. Genetic dissection of structural and functional components of synaptic plasticity. I. Fasciclin II controls synaptic stabilization and growth. *Neuron* 1996a;17:641–654. [PubMed: 8893022]
- Schuster CM, Davis GW, Fetter RD, Goodman CS. Genetic dissection of structural and functional components of synaptic plasticity. II. Fasciclin II controls presynaptic structural plasticity. *Neuron* 1996b;17:655–667. [PubMed: 8893023]
- Shakiryanova D, Tully A, Hewes RS, Deitcher DL, Levitan ES. Activity-dependent liberation of synaptic neuropeptide vesicles. *Nat Neurosci* 2005;8:173–178. [PubMed: 15643430]
- Shakiryanova D, Tully A, Levitan ES. Activity-dependent synaptic capture of transiting peptidergic vesicles. *Nat Neurosci* 2006;9:896–900. [PubMed: 16767091]
- Speese SD, Budnik V. Wnts: up-and-coming at the synapse. *Trends Neurosci* 2007;30:268–275. [PubMed: 17467065]
- Steinert JR, Kuromi H, Hellwig A, Knirr M, Wyatt AW, Kidokoro Y, Schuster CM. Experience-dependent formation and recruitment of large vesicles from reserve pool. *Neuron* 2006;50:723–733. [PubMed: 16731511]
- Wagh DA, Rasse TM, Asan E, Hofbauer A, Schwenkert I, Durrbeck H, Buchner S, Dabauvalle MC, Schmidt M, Qin G, et al. Bruchpilot, a protein with homology to ELKS/CAST, is required for structural integrity and function of synaptic active zones in *Drosophila*. *Neuron* 2006;49:833–844. [PubMed: 16543132]
- Wayman GA, Impey S, Marks D, Saneyoshi T, Grant WF, Derkach V, Soderling TR. Activity-dependent dendritic arborization mediated by CaM-kinase I activation and enhanced CREB-dependent transcription of Wnt-2. *Neuron* 2006;50:897–909. [PubMed: 16772171]
- Wu CF, Ganetzky B. Genetic alteration of nerve membrane excitability in temperature-sensitive paralytic mutants of *Drosophila melanogaster*. *Nature* 1980;286:814–816. [PubMed: 6250083]
- Wu GY, Deisseroth K, Tsien RW. Spaced stimuli stabilize MAPK pathway activation and its effects on dendritic morphology. *Nat Neurosci* 2001;4:151–158. [PubMed: 11175875]
- Yao J, Qi J, Chen G. Actin-dependent activation of presynaptic silent synapses contributes to long-term synaptic plasticity in developing hippocampal neurons. *J Neurosci* 2006;26:8137–8147. [PubMed: 16885227]
- Yoshihara M, Adolfsen B, Galle KT, Littleton JT. Retrograde signaling by Syt 4 induces presynaptic release and synapse-specific growth. *Science* 2005;310:858–863. [PubMed: 16272123]
- Yu D, Akalal DB, Davis RL. *Drosophila* alpha/beta mushroom body neurons form a branch-specific, long-term cellular memory trace after spaced olfactory conditioning. *Neuron* 2006;52:845–855. [PubMed: 17145505]
- Yu X, Malenka RC. Beta-catenin is critical for dendritic morphogenesis. *Nat Neurosci* 2003;6:1169–1177. [PubMed: 14528308]
- Yuste R, Bonhoeffer T. Genesis of dendritic spines: insights from ultrastructural and imaging studies. *Nat Rev Neurosci* 2004;5:24–34. [PubMed: 14708001]
- Zinsmaier KE, Eberle KK, Buchner E, Walter N, Benzer S. Paralysis and early death in cysteine string protein mutants of *Drosophila*. *Science* 1994;263:977–980. [PubMed: 8310297]

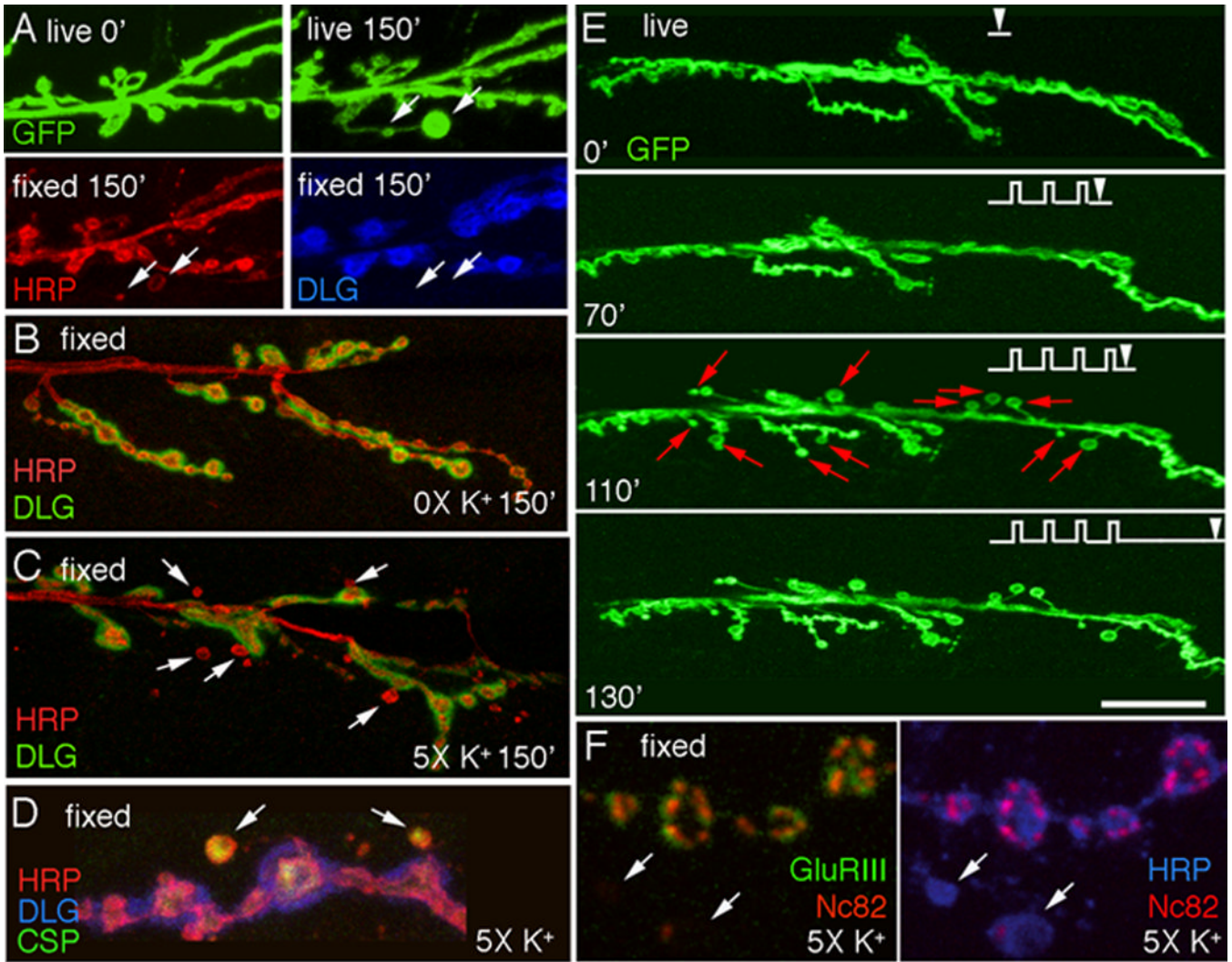
- Zito K, Parnas D, Fetter RD, Isacoff EY, Goodman CS. Watching a synapse grow: noninvasive confocal imaging of synaptic growth in *Drosophila*. *Neuron* 1999;22:719–729. [PubMed: 10230792]
- Zucker RS. Minis: whence and wherefore? *Neuron* 2005;45:482–484. [PubMed: 15721234]





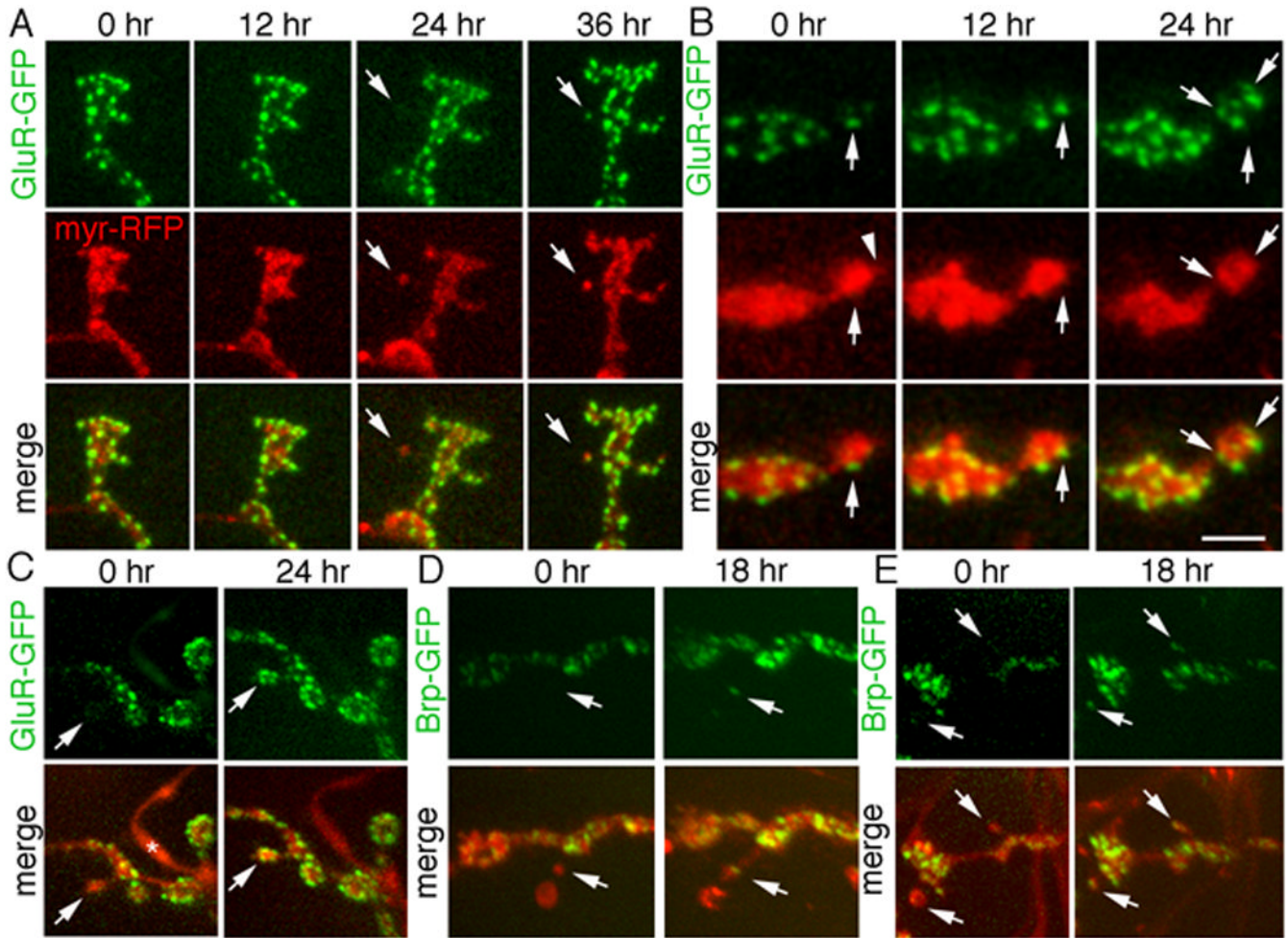
**Figure 1.**

Acute spaced stimulation induces the formation of synaptopods at the NMJ. **(A)** Time lapse images of live NMJs expressing membrane tethered GFP in motorneurons about 2.5 hr from the beginning of spaced depolarization (exact time is stated in minutes in each panel). Red arrowheads point to a retracting synaptopod. White arrowheads point to elongating synaptopods. **(B)** High K<sup>+</sup>-induced depolarization paradigms. **(C)** Number of synaptopods per NMJ arbor in wild type controls and preparations stimulated with spaced high K<sup>+</sup> depolarization. **(D)** Comparison of a representative NMJ arbor imaged live **(D1)** before and **(D2)** after 2.5 hrs from the beginning of spaced high K<sup>+</sup> depolarization, showing the increase in synaptopod frequency and length. Left column shows an entire NMJ at muscle 6 and 7, and right column is a high magnification view of the NMJ area circumscribed by the box in the left column panels. Arrows point to synaptopods. \*\* =  $p < 0.001$ . Calibration scale is 4.5  $\mu\text{m}$  in A, 23  $\mu\text{m}$  in D left column, and 5  $\mu\text{m}$  in D right column.



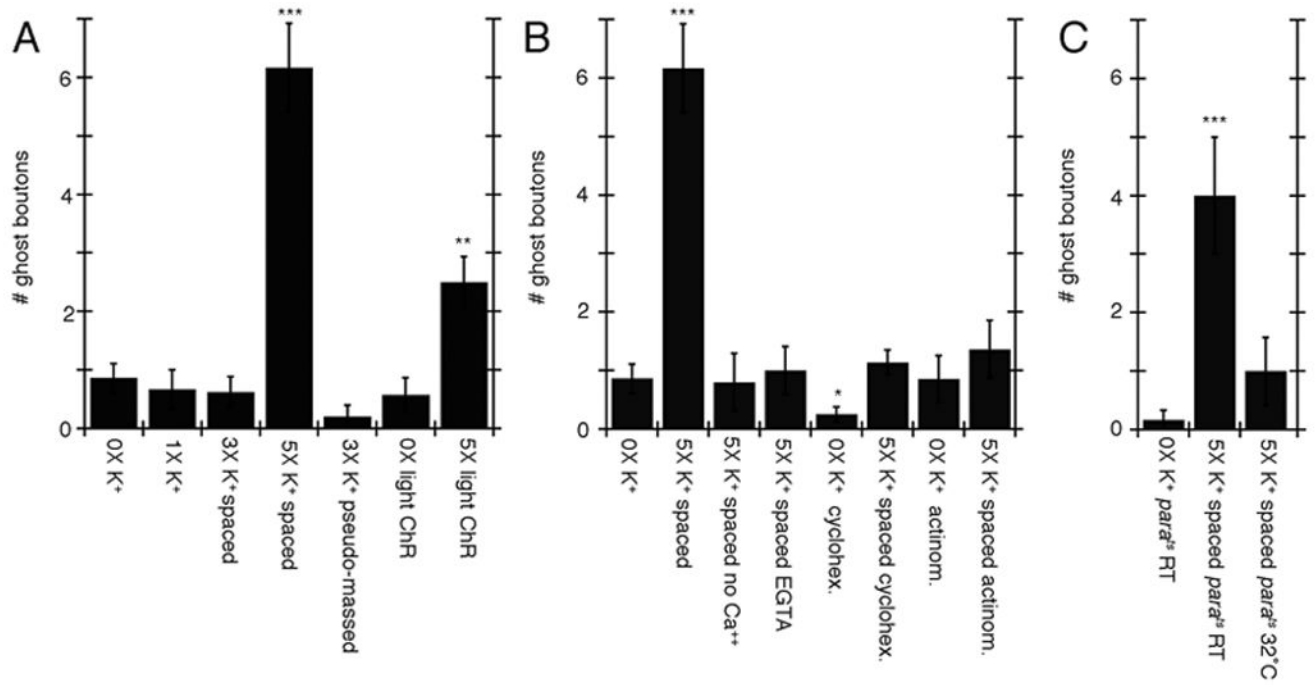
**Figure 2.**

Acute spaced stimulation induces the formation of undifferentiated “ghost boutons”. (A) *De novo* ghost bouton formation observed live, after 150 min from the beginning of spaced depolarization. In A (bottom row) the same sample shown in (A top right panel) is exhibited after fixation and immunocytochemical staining with anti-HRP (left panel) and anti-DLG (right panel) antibodies, Arrows point to two ghost boutons in the live and fixed preparations. (B, C) NMJs double stained with anti-HRP and anti-DLG antibodies in (B) a control unstimulated preparation, and (C) a sample subjected to spaced 5X K<sup>+</sup> depolarization, fixed and imaged at 2.5 hrs after dissection. Arrows in (C) point to ghost boutons, which are recognized by labeling with anti-HRP antibodies, while lacking DLG immunoreactivity. (D, F) View of ghost boutons (arrows) in preparations fixed after stimulation and triple stained with (D) HRP, DLG, and CSP antibodies showing that ghost boutons contain a synaptic vesicle marker, and (F) HRP, NC82, and GluRIII antibodies showing that ghost boutons are devoid of GluR clusters and most active zones. (E) Time-lapse image series in which the preparation was imaged before stimulation and at the indicated times during the spaced stimulation protocol (arrowheads). Note the sudden appearance of ghost boutons (red arrows) after the 4<sup>th</sup> depolarization pulse. Calibration scale is 12 μm in (A); 17 μm in (B, C); 6.5 μm in (D, F); and 24 μm in (E).



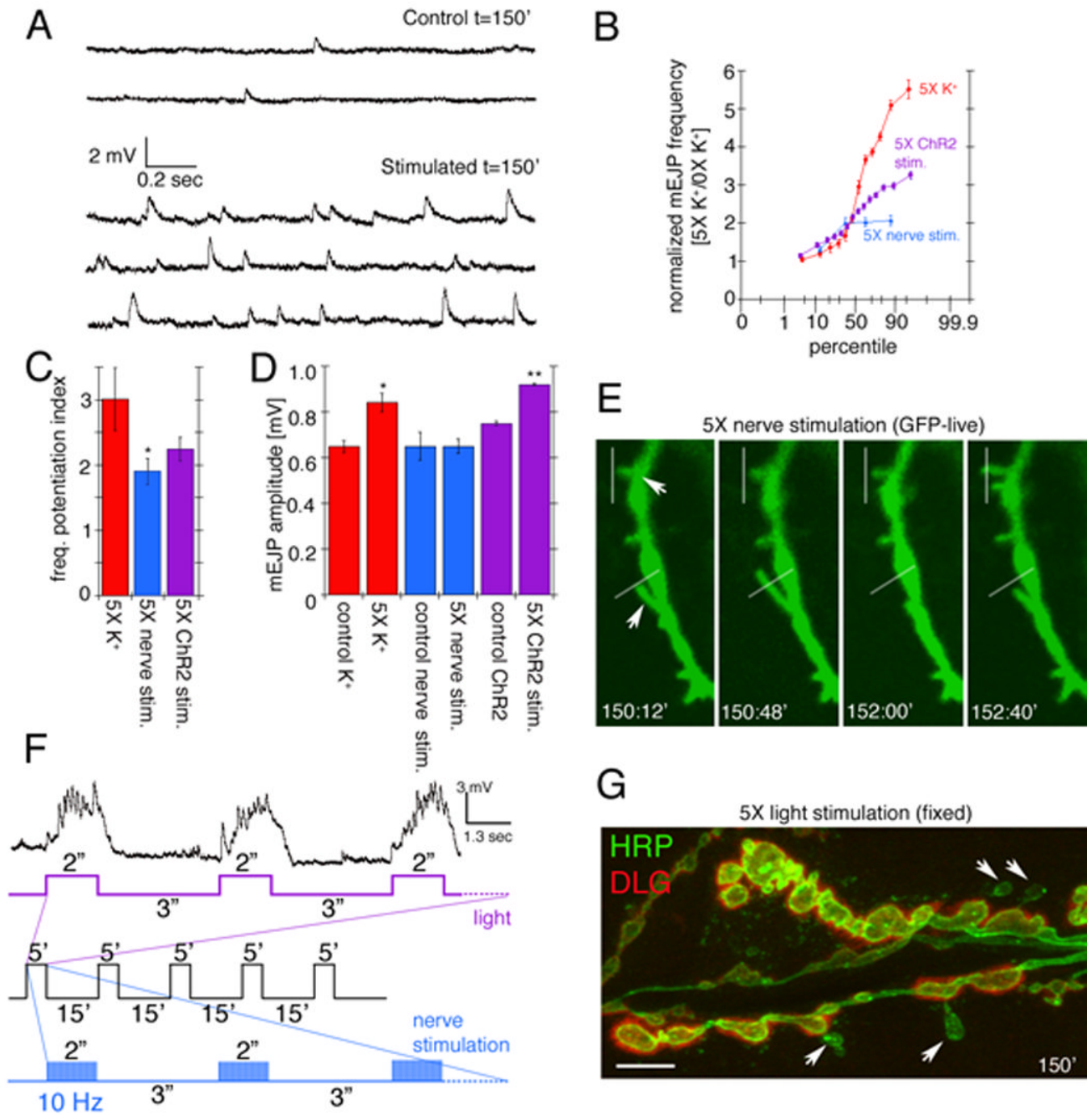
**Figure 3.**

Ghost boutons form *de novo* in intact undissected larvae and develop into mature boutons by acquiring postsynaptic GluR and presynaptic Brp clusters. Time-lapse imaging through the intact cuticle of NMJs expressing presynaptic myr-RFP (red) and either postsynaptic GluR-GFP (green) or presynaptic Brp-GFP (green) showing (A) *de novo* formation of a ghost bouton (arrows) in muscle 27 at 24hr and clustering of GluR receptors on the ghost bouton (arrows) at 36hr. (B) Progressive increase in the number of GluR clusters (arrows) in a differentiating bouton, on muscle 27, over a 24hr period. Arrowhead in myr-RFP at 0 hr points to a synaptopod (C) Another example of a ghost bouton (arrows) in muscles 14 and 30 imaged at 0hr, which acquired GluR clusters (arrows) at 24 hours. \* = peptidergic ending, which normally lacks GluR clusters. (D, E) Ghost boutons (arrows) in muscles 14 and 30 at 0hr, which acquired Brp clusters at 18 hr (arrows). Thin neurites may appear invisible, next to bright mRFP signal of boutons. Calibration scale is 5  $\mu\text{m}$  in A, 3  $\mu\text{m}$  in B, and 8  $\mu\text{m}$  in C–E.



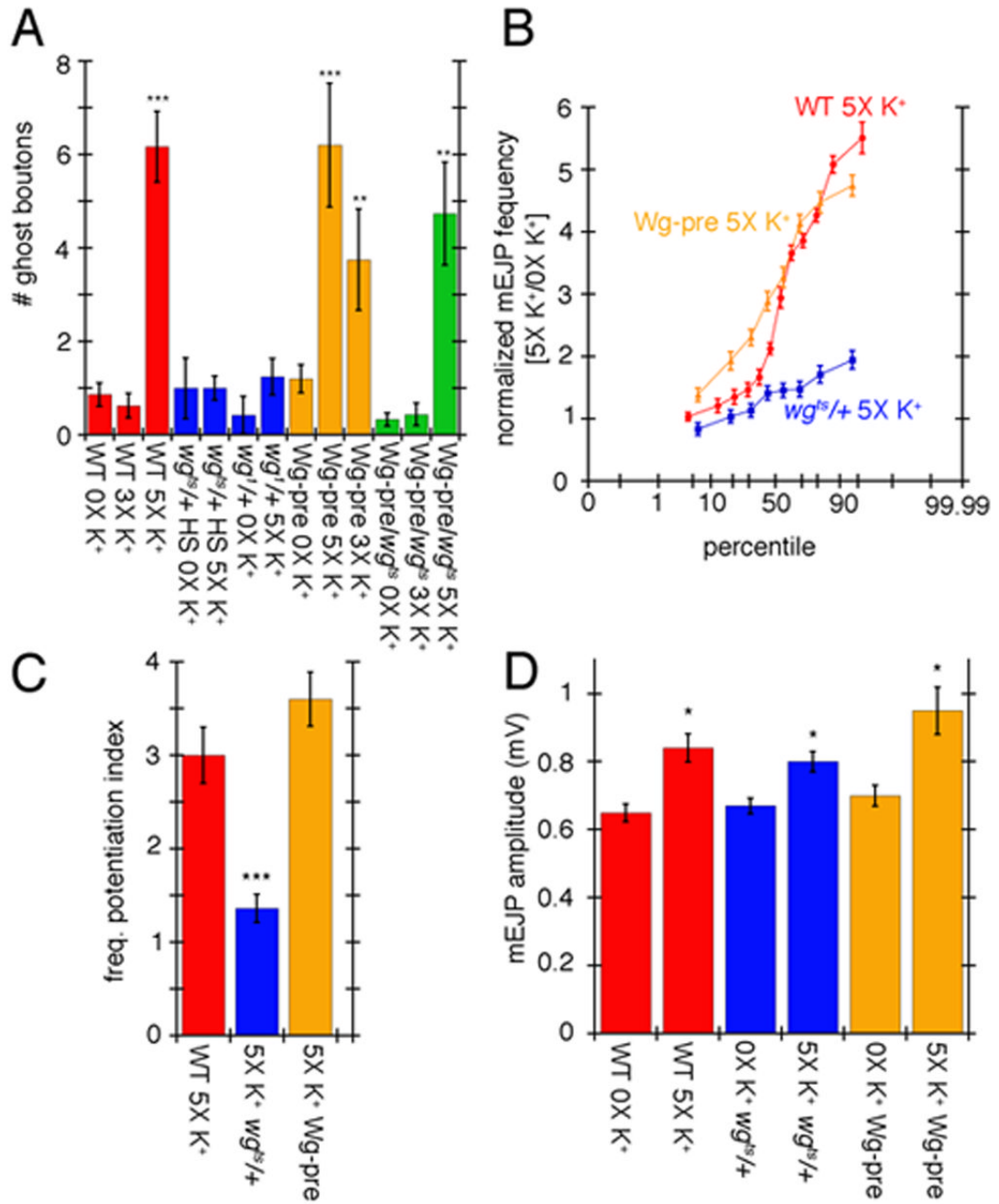
**Figure 4.**

Activity-dependent ghost bouton formation depends on spaced stimulation, Ca<sup>++</sup>, as well as transcription and translation. (A–C) Number of ghost boutons upon K<sup>+</sup> depolarization induced (A) by using alternative stimulation protocols, (B) in the presence of different drugs and Ca<sup>++</sup> conditions (no Ca<sup>++</sup> and 0.5 mM EGTA) and (C) in *para<sup>ts</sup>* mutants. \* = p < 0.05, \*\* = p < 0.001, \*\*\* = p < 0.0001.



**Figure 5.** Potentiation of spontaneous release frequency after spaced K<sup>+</sup> depolarization, nerve stimulation, and light induced stimulation of motoneurons by using ChR2. **(A)** mEJP traces in (top) controls and (bottom) samples subjected to spaced 5X K<sup>+</sup> depolarization. **(B)** Normalized probability distribution of mEJP frequencies, obtained by dividing the mEJP frequency of experimental samples by the mean control frequencies, after spaced 5X K<sup>+</sup> depolarization (red), 5X nerve stimulation (blue), or 5X light stimulation of presynaptic ChR2 (purple). **(C)** mEJP frequency potentiation index (mEJP frequency in experimental samples divided by the mean control frequency). **(D)** Mean mEJP amplitude after the above stimulation paradigms. **(E)** Paradigms for nerve and light stimulation and postsynaptic recording of

responses to the 5X light ChR2 paradigm. Traces below the recording correspond to (purple) LED lights on and off cycles and (blue) nerve stimulation, with the entire 5X paradigm shown in black. (**E**, **G**) Morphological plasticity of NMJs upon (**E**) 5X nerve and (**G**) 5X ChR2 stimulation. (**E**) shows an instance of extending and retracting synaptopods (arrows mark moving synaptopods, white lines are fiduciary markers) in a presynaptic mCD8-GFP-labeled preparation imaged live. (**G**) shows an example of enhanced ghost bouton formation (arrows) in a fixed preparation double labeled with anti-HRP (green) and anti-DLG (red) antibodies. \*= $p < 0.05$ , \*\*= $p < 0.001$ . Calibration scale is 3  $\mu\text{m}$  in E and 6  $\mu\text{m}$  in G.

**Figure 6.**

*Wg* signaling regulates ghost bouton formation and mEJP potentiation. (A) Number of ghost boutons after 0X, 3X, or 5X spaced K<sup>+</sup> stimulation in controls (red), *wg<sup>ts</sup>/+* heterozygous and *wg<sup>1</sup>* homozygous mutants (blue), upon expressing UAS-*Wg* in motorneurons (orange), and upon rescuing *wg<sup>ts</sup>* with UAS-*Wg* in motorneurons (green). (B) Normalized probability distribution of mEJP frequencies in the indicated genotypes after spaced 5X K<sup>+</sup> stimulation. Normalization was obtained by dividing the frequency of experimental samples by the mean control frequencies. (C) Frequency potentiation index. (D) Mean mEJP amplitude in the indicated genotypes in controls and samples subjected to spaced 5X K<sup>+</sup> stimulation. \* =  $p < 0.05$ , \*\* =  $p < 0.001$ , \*\*\* =  $p < 0.0001$ .

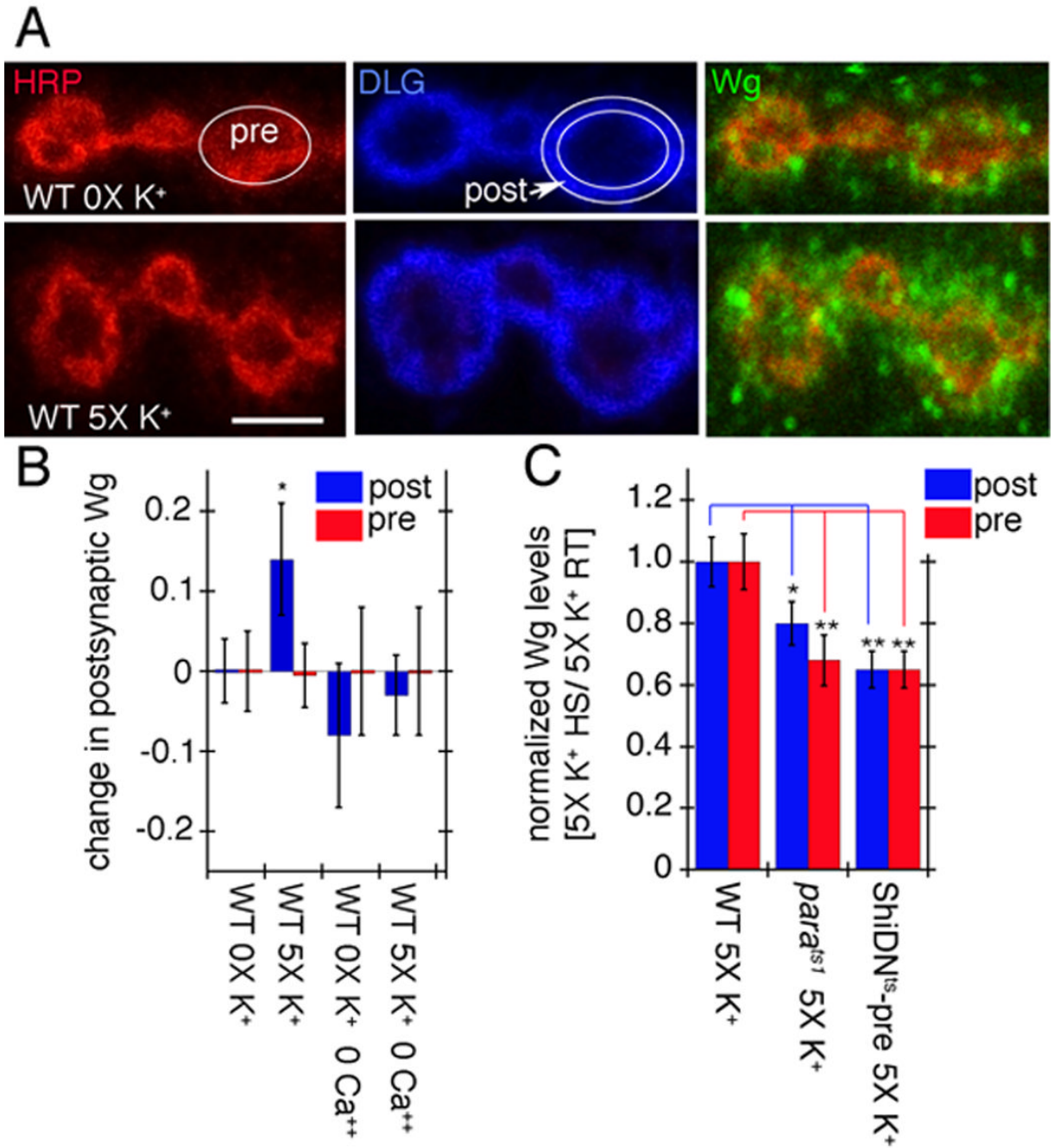


**Figure 7.**

Activity-dependent Wg secretion by synaptic boutons. (A) Wg immunoreactivity (green) at synaptic boutons of wild type (top row) controls and (bottom row) specimens subjected to spaced 5X K<sup>+</sup> depolarization in samples triple stained with anti-HRP (red), anti-DLG (blue) and anti-Wg (green). Images correspond to single confocal slices. The postsynaptic (DLG minus HRP) and the presynaptic (HRP) areas are outlined in white in the middle-upper and the left-upper rows respectively. (B) Pre- (red) and postsynaptic (blue) Wg levels in wild type controls and samples subjected to spaced 5X K<sup>+</sup> depolarization, in the presence or absence of Ca<sup>++</sup>. Numbers in the Y-axis correspond to the difference in mean Wg intensity levels between control and experimental samples. (C) Pre- (red) and postsynaptic (blue) Wg levels in response



to 5X K<sup>+</sup> depolarization after blocking activity with *para<sup>ts1</sup>* and ShiDN<sup>ts</sup>-pre. Wg levels were normalized by dividing the Wg levels after the 5X K<sup>+</sup> paradigm at restrictive temperature (HS) by the Wg levels after the 5X K<sup>+</sup> paradigm at permissive temperature (RT). Calibration scale is 2.5 μm in A.

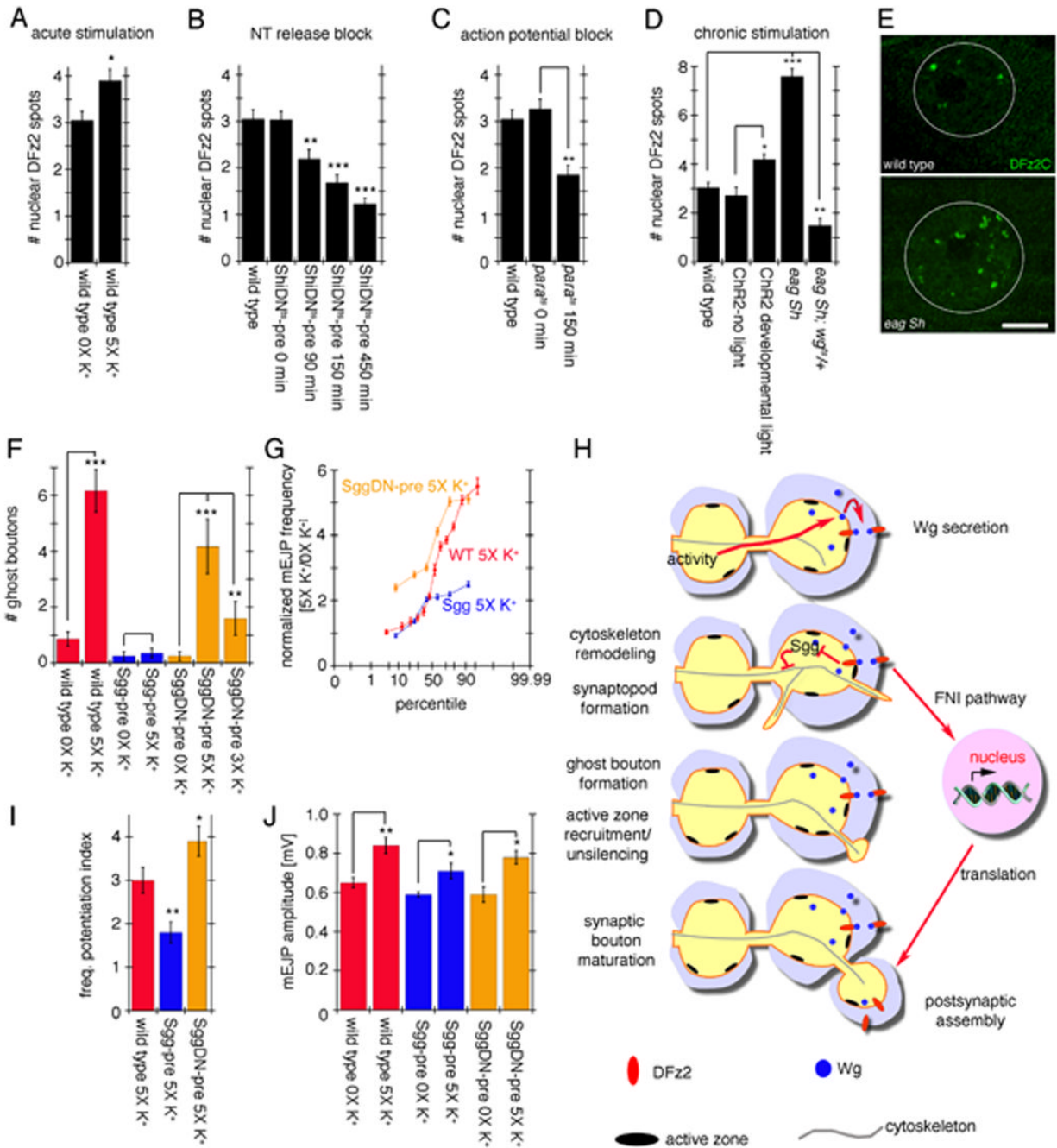


**Figure 8.** Activity-dependent regulation of postsynaptic DFz2C nuclear import and role of Sgg in rapid activity-dependent changes at the NMJ. (A–D) Number of DFz2C nuclear spots in (A) wild type after spaced 5X K<sup>+</sup> depolarization, (B) larvae expressing ShiDN<sup>ts</sup> in motorneurons and in which neurotransmitter release was blocked for 90, 150, and 450 min, (C) *para<sup>ts1</sup>* animals in which action potentials were blocked for 150 min, and (D) *eag Sh* mutants (chronic hyperexcitability) and larvae expressing ChR2 in motorneurons and stimulated by light with a developmental paradigm (see Methods). (E) Nuclear DFz2C immunoreactivity in the postsynaptic muscle nucleus of wild type (top) and *eag Sh* mutants. White circles outline the nucleus. (F, G, I, J) Effect of alterations in Sgg activity in ghost bouton number and mEJP

potentiation. **(F)** Number of ghost boutons, **(I)** mEJPs frequency potentiation index and **(J)** and mean mEJP amplitude upon spaced 5X K<sup>+</sup> stimulation in controls (red) as well as in animals overexpressing Sgg (blue) and SggDN (orange) in motoneurons. **(G)** shows the normalized probability distribution of mEJP frequencies in the above genotypes. \*= p<0.05, \*\*= p<0.001, \*\*\*=p<0.0001. Calibration scale in E is 11 μm. **(G)** Proposed model for activity-dependent regulation of synapse formation at the NMJ. Patterned activity induces Wg secretion from presynaptic terminals. Once released, Wg binds to DFz2 receptors localized both pre- and postsynaptically. In the presynaptic cell, Wg transduction leads to the formation of synaptopods and ghost boutons in part through regulation of cytoskeletal dynamics, which involves inhibition of GSK-3β/Sgg activity. In the postsynaptic cell, Wg activates the Frizzled Nuclear Import (FNI) pathway and signals the formation/stabilization of synaptic specializations through transcriptional regulation.